Received August 31, 2017, accepted September 24, 2017, date of publication October 17, 2017, date of current version November 14, 2017.

*Digital Object Identifier 10.1109/ACCESS.2017.2764056*

# A New Method for the Design of Optimal Control in the Transient State of a Gas Turbine Engine

**BING YU, CAN CAO, WENJUN SHU, AND ZHONGZHI HU**

Jiangsu Province Key Laboratory of Aerospace Power Systems, College of energy and power engineering, Nanjing University of Aeronautics and Astronautics, Nanjing 210016, China

Corresponding author: Bing Yu (yb203@nuaa.edu.cn); Zhongzhi Hu (Zhongzhi Hu@nuaa.edu.cn)

This work was supported in part by the Natural Science Foundation of China under Grant 51406083, in part by the Natural Science Foundation of Jiangsu Province under Grant BK20140820, and in part by the Fundamental Research Funds for the Central Universities under Grant NJ20160037.

**ABSTRACT** To improve the control performance in the transient state of a gas turbine engine, a new method based on variable replacement method (VRM) and particle swarm optimization (PSO) algorithm is proposed. Above all, an acceleration schedule under the constraints of fuel air ratio (*FAR*), high pressure turbine inlet temperature ($T_4$) and high pressure compressor surge margin (*SM*) could be obtained. Then PSO is employed to optimize the acceleration controller. At the same time, the deceleration controller is designed in consideration of minimum fuel ratio unit ($W_f/P_{s_3}$) limiter. At last, a simulation is carried out to verify the performance of the proposed method and the results manifest that the optimized controller can track the acceleration command quickly and accurately, while accomplish the requirement of minimum fuel ratio unit (0.005) in deceleration.

**INDEX TERMS** Transient state control, acceleration schedule, optimal control, VRM, PSO.

## Nomenclature

| | |
|---|---|
| HPC | High pressure compressor. |
| HPT | High pressure turbine. |
| LPC | Low pressure compressor. |
| LPT | Low pressure turbine. |
| ITAE | Integral of time-weighted absolute value of the error. |
| $W$ | Mass flow. |
| $W_f$ | Fuel mass flow. |
| $Ps_3$ | High pressure compressor outlet static pressure. |
| $T_4$ | Combustor outlet temperature. |
| $SM$ | Surge margin of high pressure compressor. |
| $N1$ | Fan speed. |
| $Nc$ | Core speed. |
| $PR$ | Pressure ratio. |
| $\varepsilon_i$ | Residual of co-operating equation. |
| $J_l$ | Low pressure shaft moment of inertia. |
| $J_h$ | High pressure shaft moment of inertia. |
| $BPR$ | Bypass ratio. |
| $FAR$ | Fuel air ratio. |
| $SPR$ | Pressure ratio on the surge line. |
| $Ncdot$ | Acceleration of high pressure rotor speed. |
| $LPT\_PR$ | Pressure ratio of LPT. |
| $HPT\_PR$ | Pressure ratio of HPT. |
| $Fan\_Rline$ | Rline value of fan. |
| $HPC\_Rline$ | Rline value of HPC. |
| $LPC\_Rline$ | Rline value of LPC. |
| trq | Torque. |
| max | Maximum. |
| min | Minimum. |
| cmd | Command. |
| act | Actual. |

## I. INTRODUCTION

Consider the aircraft engine is a nonlinear and complex system, its control work is a challenging task which always takes a very long time. Among this time, the transient state control design takes up nearly 3/4 of the total cycle in the development of an aircraft engine control system. It is because the transient state control should drive the engine with a good dynamic performance over a large nonlinear range, and it must protect the engine from exceeding its physical limits such as the maximum rotor speed, the maximum operating temperature of turbine blades, the maximum pressure of the combustion chamber and the stall/surge margin of compression system [1].

How to extract the acceleration potential of an aircraft engine safely has been a hot issue in the design of transient state controller. Since the 1970s, many researchers have carried out large amounts of works on it. At very beginning, most researchers successfully used linear quadratic regulator theory (LQR) or improved LQR as the control method. In 1973, GJ Michael and FA Farrar applied LQR to a nonlinear multivariable feedback controller for F401 turbofan engine. A quadratic performance index intended to minimize acceleration time was formulated, thus the feedback control gains were determined [2], [3]. To minimize the acceleration time, MS Weinberg utilized LQR to design the controller for F100 engine in 1976 [4]. To improve the acceleration performance for a turbojet engine, GJ Sevich and EC Beattie proposed an approximate minimum-time solution based on quadratic performance index. This performance index was minimized by using a conjugate-gradient search technique [5]. All the studies made use of integral, quadratic performance indices, in which both control deviations and state from some desired trajectory were penalized. The coefficients of the penalty terms were adjusted in an attempt to minimize the acceleration time. However, none of these reports can guarantee their methods produce truly minimum-time acceleration [6].

In 1977, F Teren utilized the nonlinear programming to study the optimal acceleration control. The nonlinear optimization program was used to obtain the optimal input of the open-loop system, taking the constraints into consideration directly in aero-engine acceleration [6]. The result proved the effectiveness of this approach. Since then, researchers have constrained the acceleration control as a nonlinear optimal control problem. J Liang and B Walker considered the compressor stall boundary as an important item in engine acceleration. By using the steepest descent solution, they converted the dynamics formulation of the engine to nondimensional variable while adding a penalty on terminal rotor speed [7]. G Chen and D Fan used the sequential quadratic programming (SQP) approach to optimize the acceleration control [8]. Xuefeng QI *et al*. applied the FSQP algorithm to the acceleration control of a turbofan engine based on multivariable optimal control method [9]. The approaches above have made great achievements, and these methods are still evolved by new algorithms and the computing power. However, the complexity of mathematical algorithms, the difficulty of engineering realization and the poor generality still limit its application greatly.

Since the year of 2000, some new methods have been proposed. In order to improve the control performance, Ai He *et al*. proposed a static compensator approach by considering the constraint as a windup problem, and designed the compensator with $H_2/H_\infty$ optimization method [10]. Yuchun Chen *et al*. proposed the power extraction method to design the acceleration/deceleration controller [11]. Lu Jun *et al*. proposed a fixed dynamic method for the design of the aero-engine transient state controller [12]. Using these two methods, the engine was forced to operating near or at the constraint boundaries by extracting additional residual power or acceleration from the engine rotor. Obviously, The value of extraction keep various repeatedly until the engine approached or reached the constraint boundaries before the optimal control law was finally determined. Csank Jeffrey *et al*. published "the Tool for the Turbine Engine Closed-Loop Transient Analysis (TTECTrA)" [13]. In this tool, the optimal open-loop input was obtained by increasing the change rate of fuel flow until the engine approached or reached the constraint boundaries, then the acceleration/deceleration schedule was calculated by using the optimal open-loop input. The method is simple and easy to verify in engineering, but it can not guarantee the acceleration performance. In recent years, studies on control of nonlinear system have made great achievements [14]–[17]. And nonlinear system control theory is also employed in the studies of engine control [18], [19]. However, these proposed methods are lack of validation in the real situations. Shi Yang *et al*. proposed the variable replacement method (VRM) [20]. This method is simple, accurate, and it can realize the best acceleration capability of engines. However, using VRM, the physical relations between independent variables of the engine must be analytically resolved. So this method is still complex to realize and lack of generality.

In this paper, an improved method based on VRM was proposed. Relative to VRM, the principle and improvement of this method were presented, and simulations of aero-engine acceleration/deceleration were introduced to prove its effectiveness and accuracy. Compared with the research mentioned above, the proposed method has following advantages: (1) There is no need to linearize the engine model; (2) Taking constraints into consideration directly; (3) No complex algorithm will be used; (4) Taking use of full acceleration capability of the engine; (5) The mathematical principle is very clear; (6) Compared with the original VRM, there is no need to pay attention to the functional relations between independent variables of the engine model. So the new method is much simpler to implement, and the versatility is greatly enhanced.

## II. VRM AND THE IMPROVED METHOD

### A. THE PRINCIPLE

There are several constraints in the engine transient state. The limiters in acceleration include: the minimum high pressure compressor surge margin $SM_{min}$, the maximum high pressure turbine inlet temperature $T_{4,max}$ while the combustor rich blow out fuel air ratio $FAR_{max}$; The limiter in deceleration generally is only the minimum fuel ratio unit $(W_f/Ps_3)_{\min}$.

These constraints actually limit the fuel flow applied to the engine. Taking the acceleration process as an example, the optimization objective of acceleration control is to minimize the acceleration time without violating any constraint, which is equivalent to giving the maximum fuel flow to the engine at each step under the constraints. When considering one constraint, we can obviously obtain the minimum acceleration time only if setting the engine to operating at the constraint boundary ($f = f_{max}$ or $f = f_{min}$).

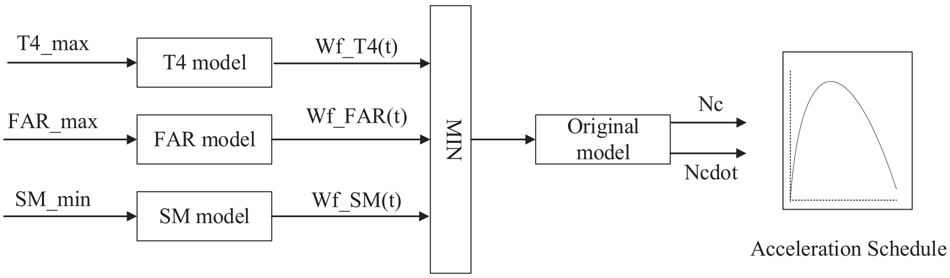


**FIGURE 1.** The flowchart of variable replacement method.

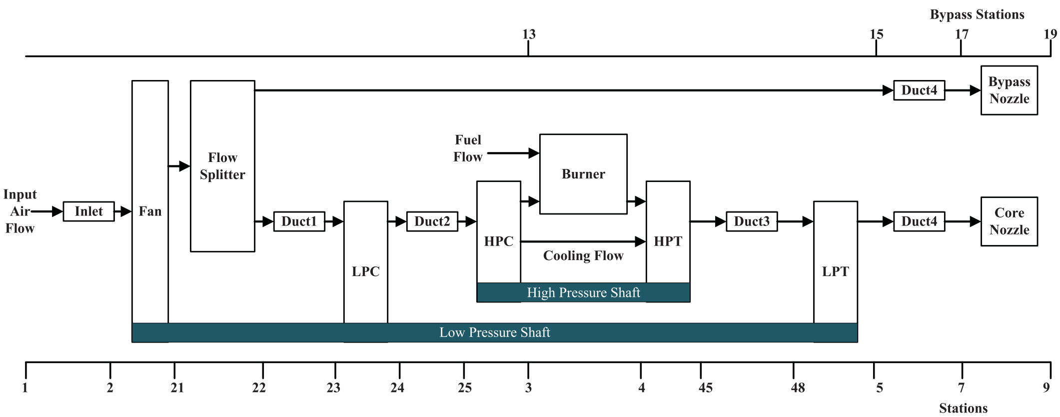


**FIGURE 2.** JT9D engine component setup.

In the standard engine model, the acceleration time is obtained by setting the value of fuel flow at each step and solving the nonlinear equations. When considering the constraint of maximum fuel air ratio $FAR_{max}$, $FAR$ can be converted into the input of the engine using a series of equations. In other words, the original model is converted into a new transient state performance calculating model with $FAR$ as its input which is called "$FAR$ model" in this paper. When the engine operates at idling initially, the input of the engine, $FAR$, will be set to the actual constraint $FAR_{max}$ at each step, and the engine will accelerate until reaching a new steady state. The acceleration and fuel flow in the process (called $W_{f,FAR}(t)$ in this paper) can be calculated at each step by solving the nonlinear equations describing the dynamic engine model. The acceleration is maximum and the acceleration schedule is optimal under $FAR$ constraint. Similarly, the $SM$ model and the $T_4$ model can be built then the $W_{f,SM}(t)$ and $W_{f,T_4}(t)$ can be obtained. When considering the three constraints, the fuel flow given to the original model will be set to $min(W_{f,FAR}(t), W_{f,SM}(t), W_{f,T_4}(t))$ at each step, then the acceleration schedule obtained is obviously the optimal acceleration control law under the three constraints. The flowchart of this method is shown in Fig. 1.

From the above analysis, the method is establishing three transient state performance calculating models. By using the dynamic JT9D engine model in the "Toolbox for the Modeling and Analysis of Thermodynamic Systems (TMATS)" as the object [21], the introduction on how to use the original method and the improved method respectively to optimize the acceleration schedule are presented in following chapters.

### B. APPLYING THE METHOD TO TMATS-JT9D

"TMATS" is a modular thermodynamic simulation package developed for the creation of dynamic simulations. It is designed as a plug-in for Simulink which allows a developer to create system simulations of thermodynamic plants (such as gas turbines) and controllers in a single tool. The JT9D dynamic engine model is a part of the tool. The structure diagram of JT9D engine is shown in Fig. 2.

The JT9D model takes fuel flow as input variable (control variable) and it has nine co-operating equations, which are Eq.1 to Eq.9.

$$(W_{21,cor} - W_{21,xcor})/W_{21,cor} = \varepsilon_1 \tag{1}$$

$$(W_{22,cor} - W_{22,xcor})/W_{22,cor} = \varepsilon_2 \tag{2}$$

$$(W_{24,cor} - W_{24,xcor})/W_{24,cor} = \varepsilon_3 \tag{3}$$

$$(W_{45,cor} - W_{45,xcor})/W_{45,cor} = \varepsilon_4 \tag{4}$$

$$(W_{5,cor} - W_{5,xcor})/W_{5,cor} = \varepsilon_5 \tag{5}$$

$$(W_{9,cor} - W_{9,xcor})/W_{9,cor} = \varepsilon_6 \tag{6}$$

$$(W_{19,cor} - W_{19,xcor})/W_{19,cor} = \varepsilon_7 \tag{7}$$

$$LPT_{trq} - Fan_{trq} - LPC_{trq} - (\frac{\pi}{30})J_L\frac{dn_1}{dt} = \varepsilon_8 \tag{8}$$

$$HPT_{trq} - HPC_{trq} - (\frac{\pi}{30})J_H\frac{dn_c}{dt} = \varepsilon_9 \tag{9}$$

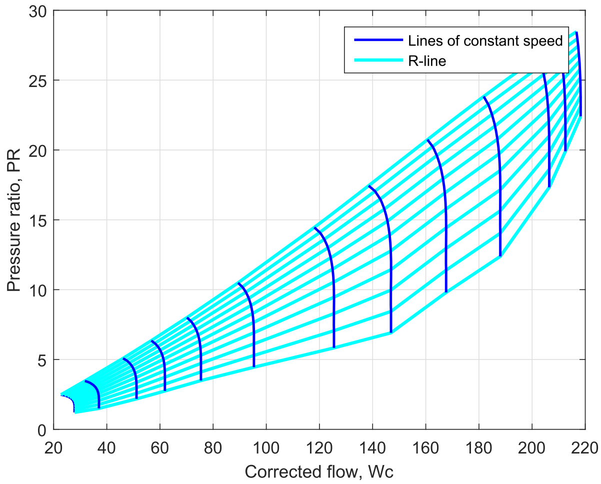


**FIGURE 3.** Engine compress component characteristics.

Corresponding to the nine co-operating equations, there are nine independent variables, $W$, $BPR$, $Fan\_Rline$, $LPC\_Rline$, $HPC\_Rline$, $HPT\_PR$, $LPT\_PR$, $N_1$, $N_c$. In Fig. 2, the definition of "Rline" is presented. The subscript "cor" represents the mass flow calculated by the independent variables $W$ and $BPR$, while the subscript "xcor" indicates the mass flow calculated through the component characteristics by the remaining independent variables. The seven flow balance equations are solved by Newton-Raphson (N-R) method, and the two power balance equations are solved by Explicit Euler method.

To sum up, the JT9D dynamic model requires ten variables to accomplish the calculation, which are $W$, $BPR$, $Fan\_Rline$, $LPC\_Rline$, $HPC\_Rline$, $HPT\_PR$, $LPT\_PR$, $N_1$, $N_c$ and $W_f$.

After the introduction for TMATS JT9D model, the optimal transient state control using the original method or the improved method can be designed.

First of all, how to establish three transient state performance calculating models by using the original method is introduced.

In TMATS-JT9D dynamic model, there are following functional relationships:

$$W_f = f_1(FAR, W, BPR) \tag{10}$$

$$W_f = f_2(T_4, W, BPR) \tag{11}$$

$$HPC\_Rline = f_3(SM, W, BPR, Nc) \tag{12}$$

In Eq. 12, $SM$ is defined as follow,

$$SM = (SPR - PR)/PR \cdot 100 \tag{13}$$

When $FAR$ limiter is considered, taking $FAR$ as the input of the model, the value of $W_f$ is calculated using Eq.10. So the $FAR$ model has all the ten independent variables needed by the original model, which means it can calculate the transient performance as the original model does. Diagram of the original method for establishing the $FAR$ model is shown in Fig. 4. The variables with "solid box" are solved by N-R method.

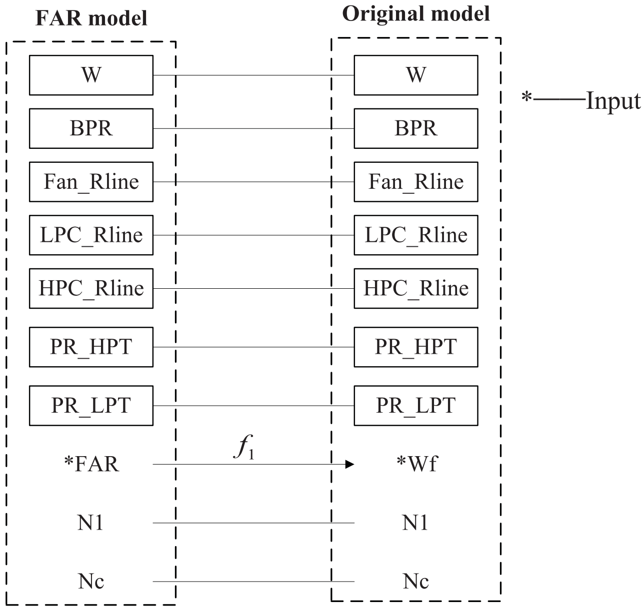


**FIGURE 4.** Diagram of the original method for establishing ***FAR*** model.

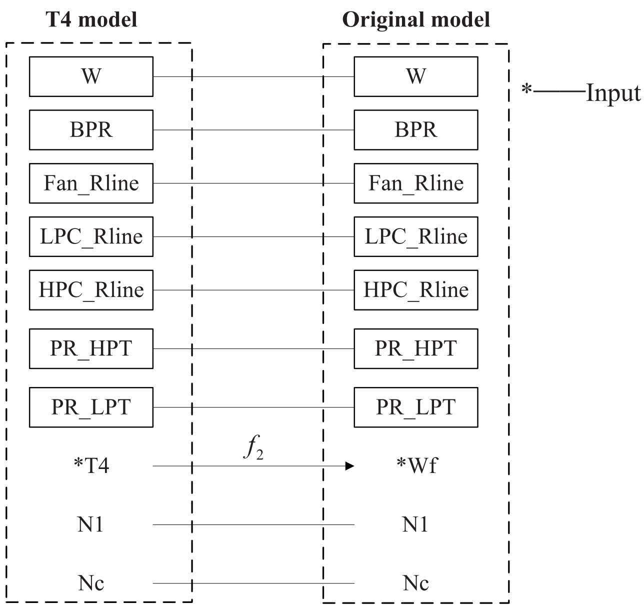


**FIGURE 5.** Diagram of the original method for establishing $T_4$ model.

Similarly, when $T_4$ and $SM$ limiters respectively are considered, the variable replacement methods are shown in Fig.5 and Fig.6, respectively.

In conclusion, when using the original method, the physical relations between different inputs of the engine must be resolved before model converting. However, these relations are often obtained by engineering experience, sometimes even no analytical solutions, but only numerical solutions. Besides, due to the different methods of modeling, these relations in different engine models are likely not the same. Therefore, the original method is not as convenient or generic as we need. So a new improved method is proposed to avoid the disadvantages.

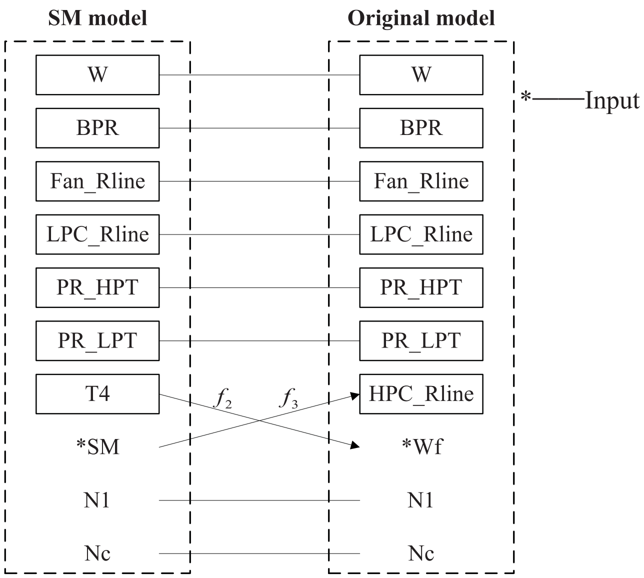


**FIGURE 6.** Diagram of the original method for establishing *SM* model.

For the proposed method, the establishment of $T_4$ model is introduced as an example.

As mentioned above, there are total ten independent variables in TMATS-JT9D dynamic model as mentioned above. So all physical parameters of the engine can be expressed as nonlinear functions of the ten independent variables in the form of:

$$y = f(X) \tag{14}$$

Where, $y$ is a physical parameter of the engine; and $X = [W, Fan\_Rline, BPR, LPC\_Rline, HPC\_Rline, HPT\_PR, LPT\_PR, N1, Nc, W_f]$.

Suppose,

$$T_4 = f_{T_4}(X) \tag{15}$$

Then, we only need to add one balance equation on the basis of the original model,

$$T_{4,cmd} - T_4 = T_{4,cmd} - f_{T_4}(X) = \varepsilon_{10} \tag{16}$$

A computational model with $T_{4,cmd}$ as input will be established, which is exactly the $T_4$ model mentioned above.

The $T_4$ model established by the new method has totally ten balance equations, which are Eq.1-9 and Eq.16.

The model takes $T_4$ as the input, and has 10 independent variables, namely, $W$, $BPR$, $Fan\_Rline$, $LPC\_Rline$, $HPC\_Rline$, $HPT\_PR$, $LPT\_PR$, $N_1$, $N_c$ and $W_f$. The two power balance equations are still solved by Explicit Euler method, and the remaining 8 flow balance equations are solved by N-R method. Similarly, the *SM* model and the *FAR* model can be established by using the new method.

From the above analysis, compared with the original method, the improved method has the following advantages: firstly, the mathematical principle is much more clearer. Secondly, because of no need to pay attention to the physical relations between different inputs of the engine, the new method is much simpler to implement, and its versatility is greatly enhanced.

### C. MODEL VERIFICATION

In this paper, the three limits in acceleration are set as $SM_{\min} = 8\%$, $T_{4,\max} = 2800°R$, $FAR_{max} = 0.024$.

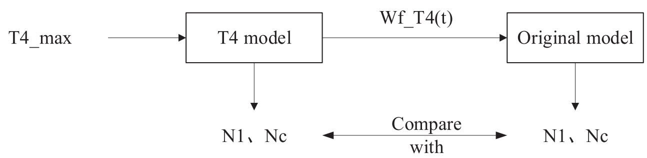


**FIGURE 7.** The validation process for $T_4$ model.

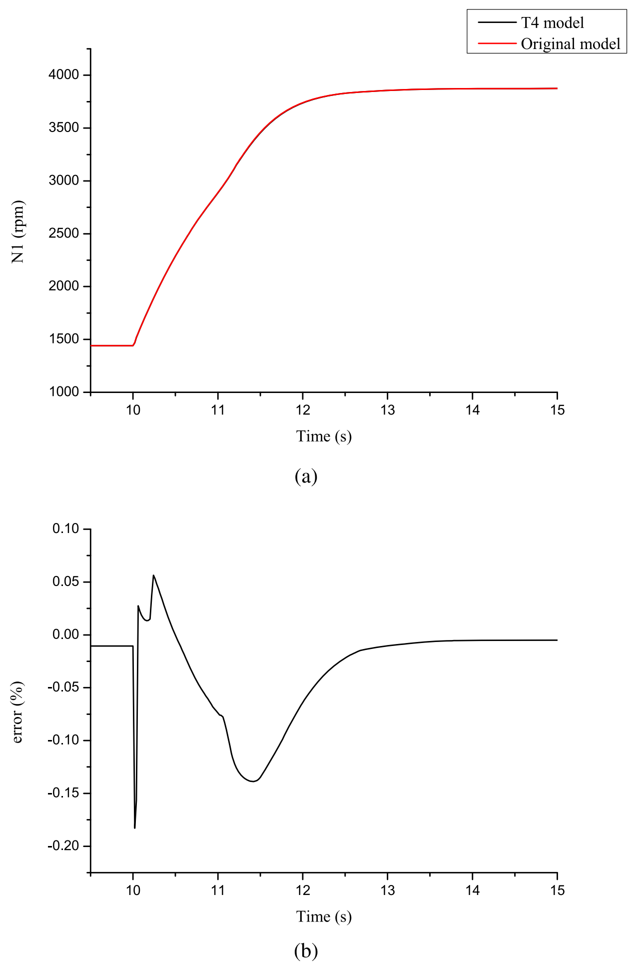


**FIGURE 8.** Comparison results of N1.

Using the improved method, three calculating models are established and validated respectively. Still taking $T_4$ model as the example, the validation process is shown in Fig. 7. Engine operates at idling initially, then $T_{4,cmd}$ is set to the limit $T_{4,max}$, engine accelerates until $T_4$ equals to $T_{4,max}$. The $W_f$ during engine acceleration, $W_{f,T_4}(t)$, can be obtained. By substituting $W_{f,T_4}(t)$ into the original model, the dynamic responses of $N1$ and $Nc$ can be obtained. Comparing them with the rotor speed dynamic responses of the T4 model, the results are shown in Fig. 8 and Fig. 9.

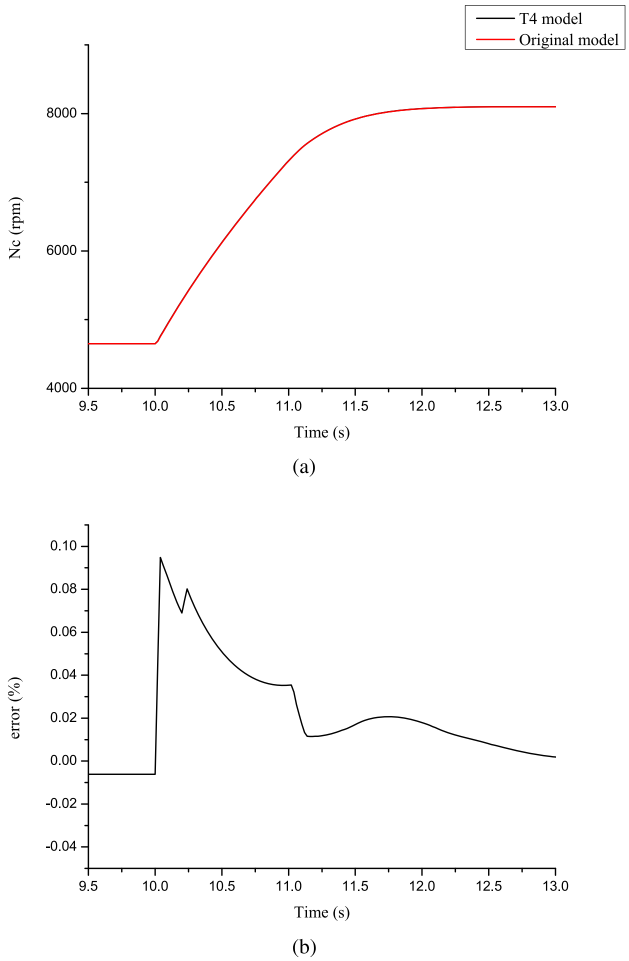


**FIGURE 9.** **Comparison results of Nc.**

It can be seen that the dynamic error of two rotor speeds does not exceed 2/1000 at worst, and the steady-state error is very close to 0 which indicate the high accuracy of $T_4$ model and the effectiveness of the improved modeling method. In addition, without considering the effect of fuel actuator, $T_4$ is always kept at the limit ($T_{4,max}$) in the whole acceleration, so maximum acceleration potential of the engine is achieved, and this will be shown in more detail in the next section by simulation results when three constraints are taken into consideration simultaneously.

The accuracy of *SM* model or *FAR* model is also high enough to meet the requirements, which is not listed here for the limited space.

### D. ACCELERATION SCHEDULE

Based on the process of the method shown in Fig. 1, using three transient state performance calculating models, the optimal acceleration schedule under the three constraints can be obtained. Meanwhile, the approach in TTECTrA is employed to determine another acceleration schedule, and the results of two methods are compared in order to verify the advantage of the proposed method.

In TTECTrA, the optimal open-loop input was obtained by increasing the change rate of fuel flow until the engine approached or reached the constraint boundaries, then the acceleration schedule was calculated by using the optimal open-loop input. Flowchart of the approach is shown in Fig. 10.

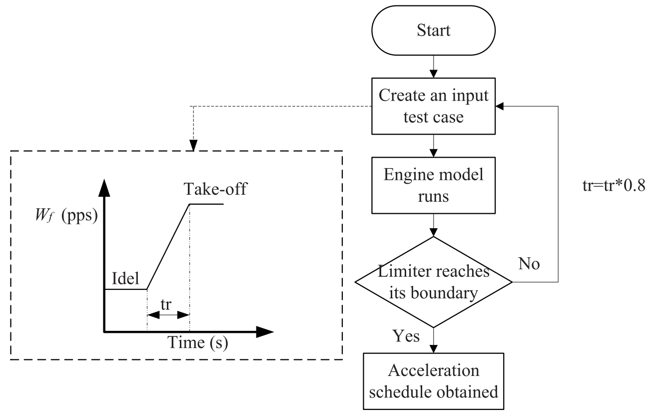


**FIGURE 10.** **Flowchart of the method in TTECTrA.**

Using these two methods, the two acceleration schedules obtained and the dynamic responses of three limiters are shown in Fig. 11.

It can be seen from Fig. 11, when using the improved VRM, each limiter approaches the constraint boundary more quickly and more approximately, therefore in the whole process the acceleration is higher than which obtained by TTECTrA method. Obviously the engine has a better dynamic performance in acceleration. In addition, we can find that the limiters are not strictly consistent with the constraints. This is because when using the proposed method, we need to take the three constraints into consideration respectively, and obtain an optimal open loop fuel flow input for each constraint. When taking the above three constraints into consideration at the same time, the fuel flow input will be set to $min(W_{f,FAR}(t), W_{f,SM}(t), W_{f,T_4}(t))$ at each step, then the acceleration schedule obtained is taken as the optimal acceleration control law under the three constraints. But, in fact, these three limiters are not independent, so using the proposed method to solve the problem is essentially an approximation. Because of the coupling of constraints, the method does not fully guarantee that the three limiters can strictly satisfy the constraints during the whole acceleration. However, because of the high nonlinearity of a gas turbine engine, it is very difficult to decouple or obtain the optimal solution. In engineering, we can use the proposed method to obtain the suboptimal solution, and then adjust the suboptimal open-loop input (or acceleration schedule) by correction and simulation so as to ensure fully satisfaction for all constraints.

## III. DESIGN OF THE ENGINE CONTROL SYSTEM

### A. ARCHITECTURE OF THE ENGINE CONTROL SYSTEM

The architecture of the engine control system used in this paper is the min/max structure, as shown in Fig. 12. Taking the minimum ($W_f/Ps_3$) limiter into consideration during the deceleration to prevent the combustor from lean blow

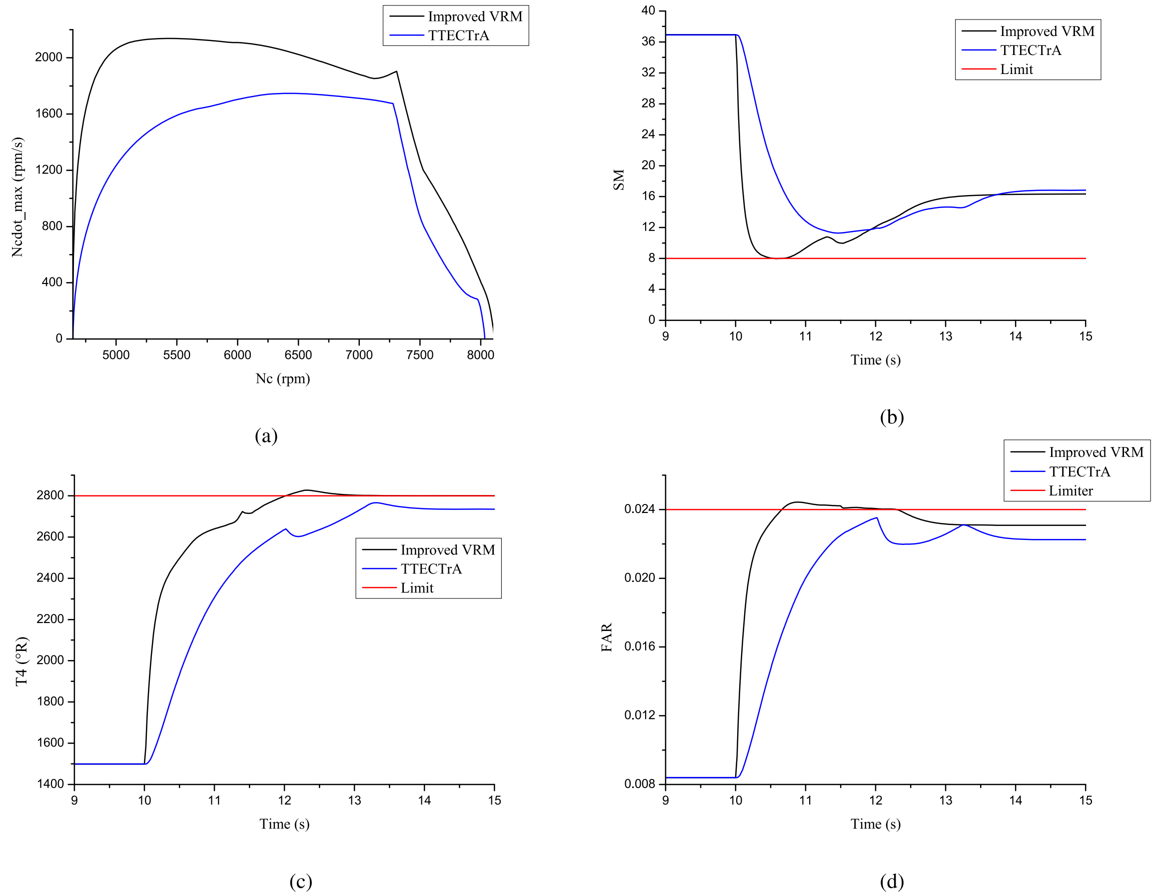


**FIGURE 11.** Acceleration schedule.

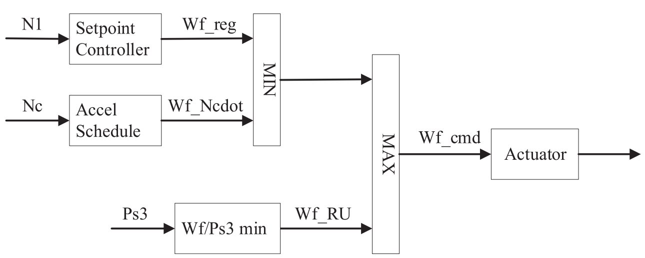


**FIGURE 12.** MIN-MAX controller architecture.

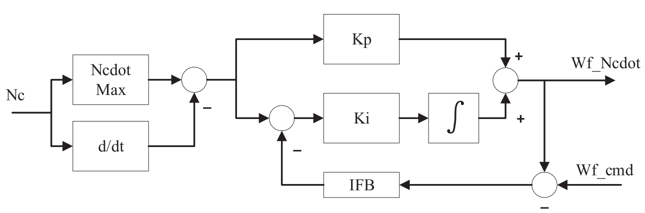


**FIGURE 13.** Acceleration schedule limiter.

out. The structure of *Ncdot* controller which is also called the "Acceleration Schedule" is shown in Fig. 13. "IFB" is the integral feedback gain used for Integral Wind-Up Protection (IWUP).

### B. PSO ALGORITHM APPLIED TO THE OPTIMIZATION OF NCDOT CONTROLLER

Particle swarm optimization (PSO) algorithm is an efficient global optimization technique, proposed by Eberhart and Kennedy in 1995 [22], [23]. It regards the design variables in the solution space as a group of "birds" (also known as "particles") and treats the optimal solution of the problem as a group looking for "food". All particles constantly change the direction and distance of flight to individual extremes and group extremes to guide themselves to adjust the flight state, which tends to the optimal solution to the problem. The update formulas of the $i$th particle of the $j$ population are as follows:

$$v_{ij}^{t+1} = \omega v_{ij}^{t} + c_1 r_1 (P_{ij,best}^{t} - x_{ij}^{t}) + c_2 r_2 (L_{ij,best}^{t} - x_{ij}^{t}) \quad (17)$$

$$x_{ij}^{t+1} = x_{ij}^{t} + v_{ij}^{t} \quad (18)$$

Where $x$ represents the current position of the particle; $v$ is the velocity of the particle; $P_{best}$ represents individual extremum; $L_{best}$ represents the extremum in neighborhood; $\omega$ is an inertial weight, which is an important parameter that affects the performance of the algorithm for its size determines how much the particle is inherited at current velocity. $c_1$ and $c_2$ are learning factors used to adjust the step length of

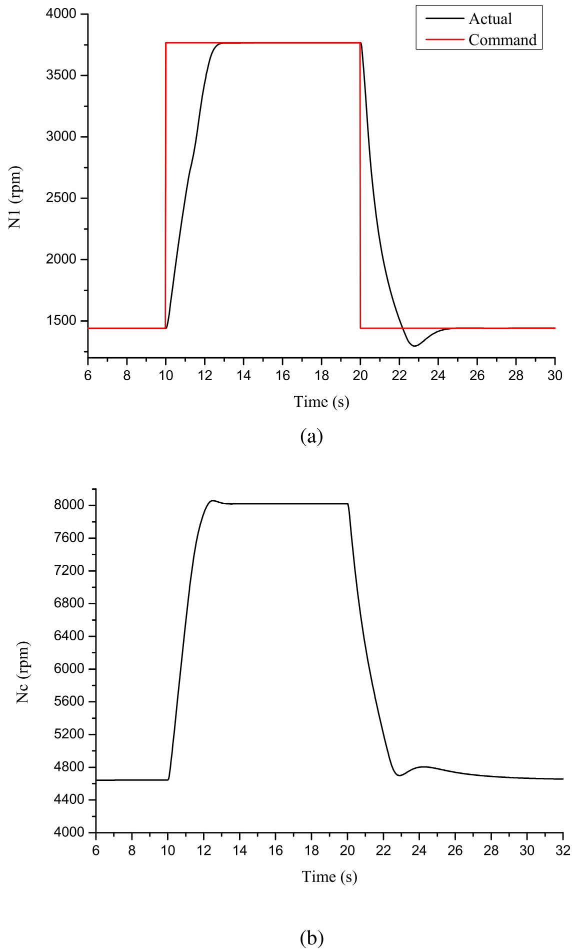


**FIGURE 14.** **Dynamic response of rotor speed.**

the particle to $P_{best}$ and $L_{best}$. $r_1$ and $r_2$ are random numbers generated between [0, 1].

In this paper, PSO is used to optimize two control gains of *Ncdot* controller, $k_P$ and $k_I$ as shown in Fig. 12. The objective function $J_i$ is the ITAE index, which is the integral criterion of time multiplication:

$$J_i = \int_{t_1}^{t_2} t\,|e(t)|dt = \int_{t_1}^{t_2} t \left| \frac{\dot{N}_{H,cmd} - \dot{N}_{H,act}}{\dot{N}_{H,cmd}} \right| dt \quad (19)$$

The fitness function $f_i$ takes its reciprocal.

$$f_i = \frac{1}{J_i} \quad (20)$$

The specific process of optimization shall not be presented here for the limited space. It shows that there is a maximum value of $f_i$ which stands for the best control effect when $k_P = 0.00677$ and $k_I = 0.22022$. So these two values are taken as the control gains of *Ncdot* controller.

### C. SIMULATION RESULTS

$N1 = 1441rpm$, $Nc = 4668rpm$ at ground idling while $N1 = 3667rpm$, $Nc = 8021rpm$ at ground take-off.

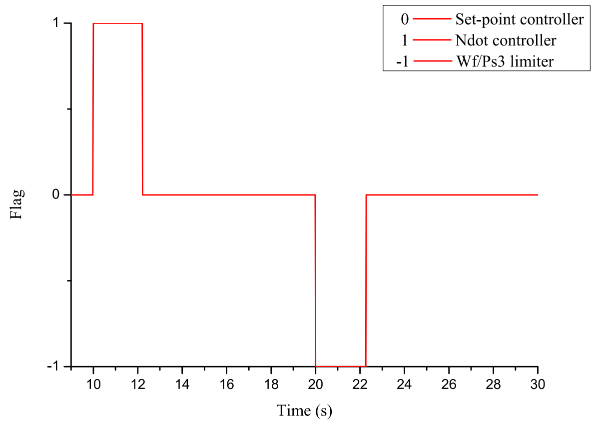


**FIGURE 15.** **Dynamic response of the flag.**

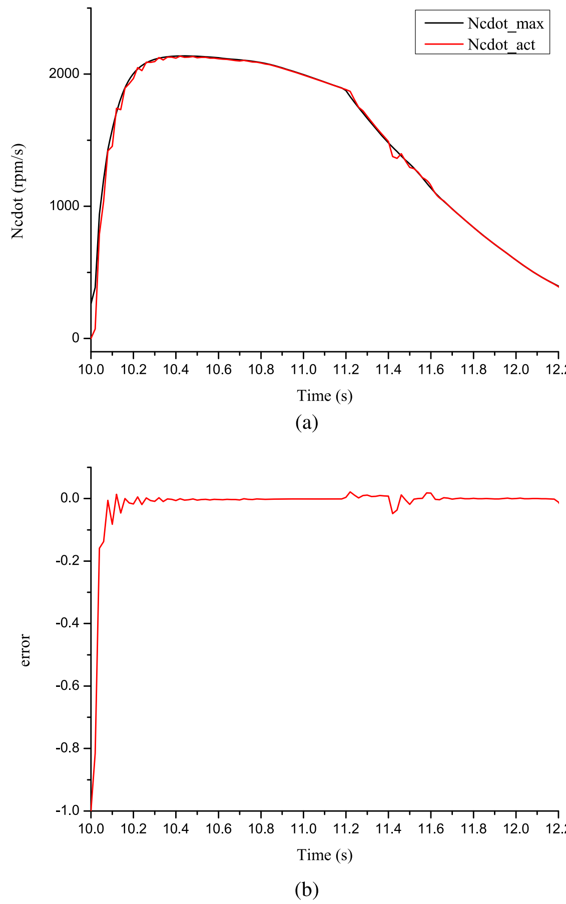


**FIGURE 16.** **The control effect of Ncdot controller.**

The JT9D engine initially operates at ground idling. $N1_{cmd}$ is set to take-off speed at 10s, and back to idling speed at 20s. The dynamic responses of $N1$ and $Nc$ in the whole process are shown in Fig. 14.

Set a flag to identify the active controller. "0" represents for the set-point controller, "1" for the *Ncdot* controller and "−1" for the deceleration controller. The response of flag is shown in Fig. 15. As can be seen, the controller switches twice either in the acceleration or in the deceleration, which is the ideal condition. There will be no multiple switches.

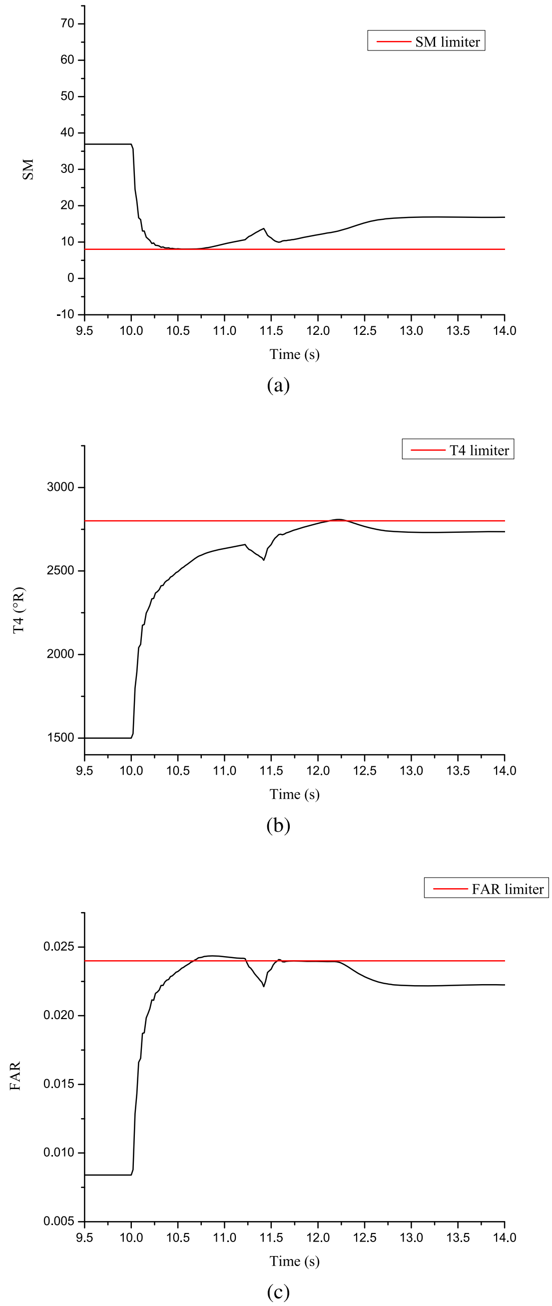


**FIGURE 17.** Dynamic response of the limiters in acceleration.

In the acceleration, the *Ncdot* controller is active from 10s to 12.2s. After that the set-point controller becomes active to control the engine to be stable at ground take-off. Analyzing the control effect of *Ncdot* controller from 10s to 12.2s, the result is shown in Fig. 16.

As can be seen from Fig. 16, under the control of *Ncdot* controller, the acceleration of rotor speed can catch the acceleration command in 0.2s, and then accurately track the command in the whole acceleration process. The dynamic error is less than 5% at worst while being maintained in the vicinity of 0 most of the time with no overshoot basically.

In the acceleration, the dynamic responses of *FAR*, *SM*, and $T_4$ are shown in Fig. 17.

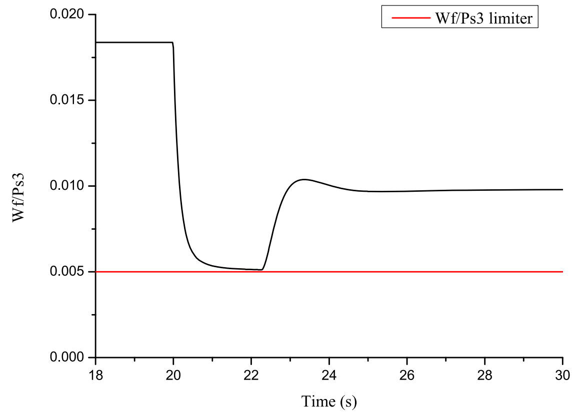


**FIGURE 18.** Dynamic response of $W_f/Ps_3$ in deceleration.

It can be seen from Fig. 17 that all the limiters can extremely approach or reach the constraints with no exceeding basically in the acceleration. To sum up, it is effective and accurate to design the optimal acceleration schedule by using the improved method based on VRM. As mentioned above, we have already taken the minimum ($W_f/Ps_3$) limiter into consideration to prevent combustor from lean blow out in deceleration. The dynamic response of $W_f/Ps_3$ is shown in Fig. 18.

As can be seen, the minimum value of $W_f/Ps_3$ approaches to the constraint boundary with no exceeding at all, proving the effectiveness of the deceleration controller.

## IV. CONCLUSION

A new method for the design of optimal control in the transient state of a gas turbine engine is presented in this paper. The principle and flowchart of the method are introduced. Improvement on the establishment of three transient state performance calculating models which is the core technique of the method is introduced, and its effectiveness and accuracy has been verified. Then PSO algorithm is used to optimize the acceleration controller, the simulation results show that the optimized controller can track the acceleration command rapidly and accurately. Besides, the dynamic responses of three limiters in engine acceleration are presented, it shows that all the limiters can extremely approach or reach the constraints boundary with no exceeding basically, so the effectiveness and accuracy of the new method for the design of optimal control in the transient state of aero-engine is proved. At last, the deceleration controller is designed in consideration of minimum fuel ratio unit ($W_f/Ps_3$) limiter to accomplish the controller of aero-engine transient state.

## REFERENCES

[1] L. C. Jaw and J. D. Mattingly, *Aircraft Engine Controls: Design, System Analysis, and Health Monitoring*. Washington, DC, USA: AIAA, 2009.

[2] G. J. Michael and F. Farrar, "An analytical method for the synthesis of nonlinear multivariable feedback control," United Aircraft Res. Lab., Tech. Rep. M941338-2, 1973.

[3] G. J. Michael and F. A. Farrar, "Development of optimal control modes for advanced technology propulsion systems," United Aircraft Res. Labs, East Hartford, CT, USA, Tech. Rep. UARL-N911620-2, 1974.

[4] M. S. Weinberg, "A multi-variable control for a turbofan engine operating at sea level static," in *Proc. ASME Int. Gas Turbine Fluids Eng. Conf.*, 1976, pp. 1–10.

[5] G. J. Sevich and E. C. Beattie, "Integrated flight/propulsion control design techniques starting with the engine," SAE Tech. Paper 740481, 1974.
[6] F. Teren, "Minimum time acceleration of aircraft turbofan engines by using an algorithm based on nonlinear programming," in *Proc. Joint Autom. Control Conf.*, San Francisco, CA, USA, Jun. 1977, p. E-9115, paper NASA-TM-X-73624.
[7] J. X. Liang and B. Walker, "Constrained nonlinear optimal jet engine acceleration control," in *Proc. 24th Joint Propul. Conf.*, 1988, p. 3178.
[8] G. Chen and D. Fan, "Application of SQP to acceleration control of turbofan engine," *J. Aerosp. Power*, vol. 14, no. 3, pp. 313–316, 1999.
[9] Q. I. Xue-Feng, F. Ding, Y. C. Chen, and L. I. Wei-Gang, "Multivariable optimal acceleration control of turbofan engine based on FSQP algorithm," *J. Propuls. Technol.*, vol. 25, pp. 233–236, Jun. 2004.
[10] A. He, D. Tan, and X. Wang, *et al.*, An LMI-based anti-windup design for acceleration and deceleration control of jet engines using the $H_2/H_\infty$ optimization," in *Proc. 47th AIAA/ASME/SAE/ASEE Joint Propul. Conf. Exhibit.*, 2011.
[11] C. Yuchun, L. Zhende, Y. Ning, and Y. Shouzhi, "A new method of acceleration control law design for turbine engines," *Acta Aeronautica Astron. Sinica-A, B*, vol. 29, no. 2, p. 327, 2008.
[12] L. U. Jun, Y. Q. Guo, and W. Lei, "A new method for designing optimal control law of aeroengine in transient states," *J. Aerosp. Power*, vol. 27, no. 8, pp. 1914–1920, 2012.
[13] J. Csank and A. M. Zinnecker, "Application of the tool for turbine engine closed-loop transient analysis (TTECTrA) for dynamic systems analysis," in *Proc. AIAA/ASME/SAE/ASEE Joint Propuls. Conf.*, 2015, pp. 1–16.
[14] D. Wang, J. Huang, W. Lan, and X. Li, "Neural network-based robust adaptive control of nonlinear systems with unmodeled dynamics," *Math. Comput. Simul.*, vol. 79, no. 5, pp. 1745–1753, 2009.
[15] H. Wang *et al.*, "Adaptive fuzzy decentralized control for a class of strong interconnected nonlinear systems with unmodeled dynamics," *IEEE Trans. Fuzzy Syst.*, to be published.
[16] X. Zhao, P. Shi, X. Zheng, and L. Zhang, "Adaptive tracking control for switched stochastic nonlinear systems with unknown actuator dead-zone," *Automatica*, vol. 60, pp. 193–200, Oct. 2015.
[17] X. Zhao, H. Yang, W. Xia, and X. Wang, "Adaptive fuzzy hierarchical sliding-mode control for a class of MIMO nonlinear time-delay systems with input saturation," *IEEE Trans. Fuzzy Syst.*, vol. 25, no. 5, pp. 1062–1077, Oct. 2017.
[18] J. Wang, Z. Ye, Z. Hu, X. Wu, G. Dimirovsky, and H. Yue, "Model-based acceleration control of turbofan engines with a Hammerstein-Wiener representation," *Int. J. Turbo Jet Engines*, vol. 34, no. 2, pp. 141–148, 2015.
[19] B. Yu, Y. Gao, and J. Wang, "Nonlinear control study on aircraft engine using a generalized minimum variance approach," *Adv. Mech. Eng.*, vol. 8, no. 9, p. 1687814016667383, 2016.
[20] Y. Shi, Q. Y. Tu, Y. H. Cai, C. Qiu, and Z. Y. Tan, "Optimum design method of acceleration and deceleration control schedule for gas turbine engine," *Hangkong Dongli Xuebao/J. Aerosp. Power*, vol. 28, no. 11, pp. 2567–2571, 2013.
[21] J. W. Chapman, T. M. Lavelle, J. S. Litt, and T.-H. Guo, "A process for the creation of T-MATS propulsion system models from NPSS data," in *AIAA Propulsion and Energy Forum*. Washington, DC, USA: AIAA, 2014.
[22] R. Eberhart and J. Kennedy, "A new optimizer using particle swarm theory," in *Proc. Int. Symp. MICRO Mach. Human Sci.*, 2002, pp. 39–43.
[23] J. Kennedy and R. Eberhart, "Particle swarm optimization," in *Proc. IEEE Int. Conf. Neural Netw.*, vol. 4. Nov./Dec. 1995, pp. 1942–1948.


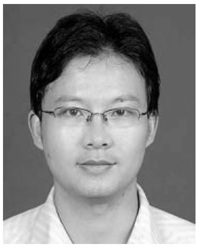

**BING YU** received the B.S. degree in automation and the Ph.D. degree in navigation guidance and control from Southeast University, China, in 2002 and 2009, respectively. He is currently an Associate Professor with the Nanjing University of Aeronautics and Astronautics. His research interests are in control and testing of the aircraft engine.

**CAN CAO** received the B.S. degree in vehicle engineering from the Nanjing University of Aeronautics and Astronautics, China, in 2012.

He is currently pursuing the master's degree in power machinery and engineering with the University of Aeronautics and Astronautics.

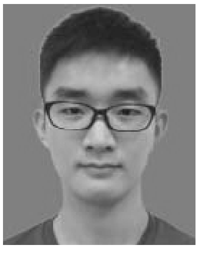

**WENJUN SHU** received the B.S. degree in flight vehicle propulsion engineering from the Nanjing University of Aeronautics and Astronautics, China, in 2016.

He is currently pursuing the master's degree in power machinery and engineering with the University of Aeronautics and Astronautics.

**ZHONGZHI HU** received the B.S. degree in automatic control from the Beijing Institute of Technology, China, the M.S. and Ph.D. degrees in electrical engineering from the University of British Columbia, Canada. He is currently Professor with the Nanjing University of Aeronautics and Astronautics, Nanjing, China. As a Researcher and an Engineer, he has over 30 years of extensive experience in modeling and simulation, controls, and PHM for gas turbine, wind turbine, and other industry applications, including 15 years of Research and Development and engineering positions involved with General Electric.

Dr. Hu published over 40 refereed conference and journal papers, and holds five U.S. patents. His research interests are in gas turbine modeling, simulation, controls, and PHM.